Surface & Coatings Technology 241 (2014) 45–49

Contents lists available at ScienceDirect

Surface & Coatings Technology

journal homepage: www.elsevier.com/locate/surfcoat

Numerical optimization of baffles for sputtering optical precision filters ☆

Andreas Pflug *, Michael Siemers, Thomas Melzig, Daniel Rademacher, Tobias Zickenrott, Michael Vergöhl

Fraunhofer Institute for Surface Engineering and Thin Films IST, Bienroder Weg 54e, 38108 Braunschweig, Germany

ARTICLE INFO

Available online 15 November 2013

Keywords:
Process modeling
Optical precision coatings
Direct Simulation Monte Carlo
Magnetron sputtering

ABSTRACT

The optimization of the coating uniformity of precision optical filters generally is a critical and time consuming procedure. The present paper demonstrates this optimization procedure on a new optical precision sputter coater "Enhanced Optical Sputtering System (EOSS)" at Fraunhofer IST. The coater concept is based on dual cylindrical sputtering sources and a rotating turn-table as sample-holder. For compensating non-uniformity introduced by the particle flux profile and the radially dependent track speed on the turntable, baffle elements have to be designed and inserted beneath the substrates.

For that purpose the distribution of the particle flow from the cylindrical magnetron as well as the resulting thickness profile for different shaper designs is simulated using Direct Simulation Monte Carlo (DSMC) transport simulation. For comparison, experimentally obtained film thickness profiles are evaluated by spectrophotometry and ellipsometry. The simulation model is used for optimization of the baffle geometry as well as investigation on the role of long term drifts caused by target erosion and mechanical tolerances.

© 2013 Elsevier B.V. All rights reserved.

1. Introduction

Advanced optical precision applications such as spectroscopy, life sciences or fsec lasers require coatings with high quality and precision. Due to the high number of layers, optical filters are quite sensitive to layer optical thickness errors; thus many products require maintaining film thickness deviations below ±0.5% or even better. With the trend of increasing substrate sizes the fabrication of such products becomes more and more a challenge.

Recently, the so-called "Enhanced optical sputtering system" (EOSS) — a novel coater concept for deposition of dielectric layers with high long-term stability and low absorption and particle contamination levels — has been introduced [1]. This coater consists of two compartments with dual rotatable sputter cathodes in a sputter-up configuration. A third compartment is equipped with an ICP source for plasma oxidation. Up to 10 substrates with a diameter of up to 200 mm can be mounted on a turntable above the sputter sources with a maximum rotation speed of 250 rpm.

Due to the radial dependency of the track speed of the turntable, the deposition rate on the substrates would decrease inversely with radial position. A baffle mounted between substrate and sputter source with appropriate geometry serves as uniformity mask for compensating this effect. Since the flux of sputtered particles is not evenly distributed on the substrate plane, the proper design of the baffle usually requires numerous deposition experiments and iterations for fine-tuning. As an alternative, this work demonstrates a method of numerically optimizing the baffle.

2. Simulation setup

The numerical optimization is accomplished by computing the flux of gas and sputtered metal within the sputter recipient. The description of particle transport under rarefied gas flow conditions is possible via the "Direct Simulation Monte Carlo" (DSMC) method [2], whereof we use an in-house developed, massive parallel implementation [3,4].

The geometric model of the sputtering recipient as shown in Fig. 1 comprises dual rotatable targets, gas inlets mounted at left and right sides, shutters, the turntable, and the baffle elements mounted just 2 mm beneath the turntable. It is assumed that the planar substrates are aligned in-line with the lower plane of the turntable.

All inner chamber surfaces relevant for gas and metal transport are represented by triangularly meshed surfaces. The geometric model and the mesh are constructed using the open source mesh generator GMSH [5].

For the sputter sources, the race tracks on the sputtering targets are approximated by four elongated rectangles (see Fig. 2). This is possible since with a target length of 550 mm and a substrate diameter of 200 mm, the end blocks have no significant contribution to the film deposited on the substrate. The target to substrate distance depends on the actual thickness of the target material and is in the range of 80 mm.

The angular and energy distribution of the sputtered particles is non-thermal and obeys a so-called Thompson energy distribution with

$$f(E,\theta) = \cos^n(\theta)\frac{E}{(E+U_b)^3} \tag{1}$$

where E is the energy, θ the polar emission angle, n is an index of the cosine angular distribution, and U_b is the binding energy of the material at the target surface.

☆ This manuscript is based on work presented at the Society of Vacuum Coaters 56th Annual Technical Conference in Providence, Rhode Island, April 20-25, 2013.

* Corresponding author.
E-mail address: andreas.pflug@ist.fraunhofer.de (A. Pflug).

0257-8972/$ – see front matter © 2013 Elsevier B.V. All rights reserved.
http://dx.doi.org/10.1016/j.surfcoat.2013.11.008

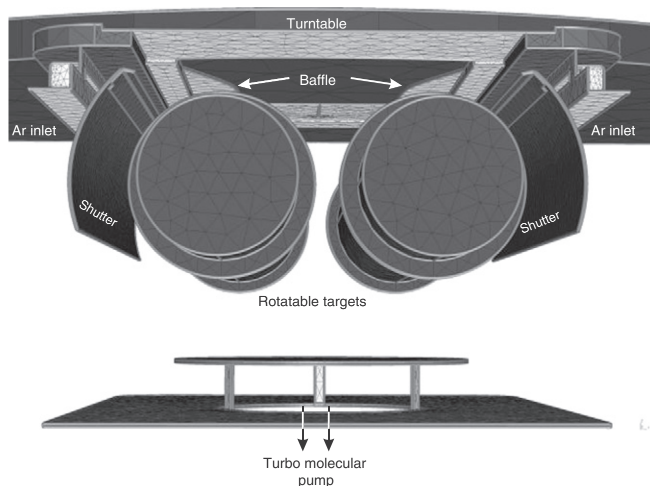

Fig. 1. Scheme of the geometry of a sputter compartment within the EOSS optical precision coater.

These data are strongly material dependent and can be found in literature e. g. in Ref. [6] or by applying Monte Carlo simulations of the collision cascade in the targets by using simulation packages such as SRIM [7]. The right graph of Fig. 2 shows the energy distribution of sputtered Nb in comparison with a Maxwellian distribution with the same maximum in energy.

The angular positions of the race tracks have been previously determined by magnetic field computation: The maximum plasma density occurs at positions, where the normal component of the magnetic field with respect to the target surface becomes zero.

With a background Ar gas pressure in the range of 300 mPa, the mean free path is in the order of 1–2 cm. Hence, to maintain proper collision statistics in the DSMC simulation, a cell dimension of about 8 mm is sufficiently small. In the actual DSMC simulation case, the geometric model is embedded into a large cuboid volume sized $1060 \times 1226 \times 635$ mm^3, the number of cells in X, Y and Z direction are 128, 150, and 80. It shall be noted that the triangular surface mesh elements visible in Figs. 1 and 2 are only relevant in the particle trajectory computation. Unless the geometric shape becomes distorted by very large elements, their size has no impact on the simulation.

For parallelization, the whole volume is sub-divided into 80 cuboid segments; a load balance algorithm measures the approximate CPU load of each segment and performs a proper assignment of volume segments to CPU cores. By this way, a good parallelization efficiency in the range of >70% is obtained for up to 40 CPU cores.

The time step used in the DSMC iterations is 1 μs implying a mean travelling path of a thermalized Ar atom of about 0.4 mm per iteration; for sputtered Nb with a kinetic energy of 10 eV, the travelling distance would be 5 mm. Thus, high energetic sputtered species are a limiting factor for the maximum possible iteration time step.

The statistical weighting factors of Ar and Nb are 3×10^{12} and 10^{10}, respectively; i.e. one Nb simulation particle represents 10^{10} real Nb atoms. A homogeneous Ar pressure distribution of 320 mPa was initially applied to the whole simulation volume. After about one real time second corresponding to 10^6 DSMC iterations the gaseous and metal flux profiles are in equilibrium. For the actual computation we use a Linux cluster based on four computing nodes whereof each is equipped with four 12-core AMD "Magny-Cours 6172" CPUs. One DSMC simulation run typically uses 30–40 cores and overall computation times between 18 and 24 hours.

For better statistics of the resulting profiles, the simulation data are time-averaged over a further time interval of 0.2 s. Cut plane views of the resulting Ar and Nb fluxes through the reactor are shown in left and center picture of Fig. 3. With respect to baffle optimization, the most relevant result from the simulation is the cumulated Nb deposition profile onto the non-shaded area of the turntable, as shown in the right picture of Fig. 3. Besides the substrate plane, also parasitic deposition onto the baffles and onto other inner chamber walls can be visualized from the simulation data. By integration over all deposited surfaces, the fraction of material which is effectively used for deposition can be evaluated.

3. Optimization method

If the baffle is located close to the substrate, it can be assumed that no significant metal–gas interaction occurs between baffle and substrate. In this case, it is a valid approach to simply cut the metal flux towards the substrate according to the baffle geometry.

The benefit of this approach is that we need only one time-consuming DSMC computation without baffles for obtaining the whole metal flux profile at the substrate plane and can subsequently compute the radial deposition profile within a simple interpolation and cutting algorithm based on the baffle geometry. The latter step only takes a few milliseconds on a single CPU; this enables to perform a systematic optimization of the baffle geometry for uniform deposition profile according to the overall scheme shown in Fig. 4. For that purpose, the inner boundary of the baffle elements is assembled from multiple circular arcs, whereof the junction coordinates and radii can be freely

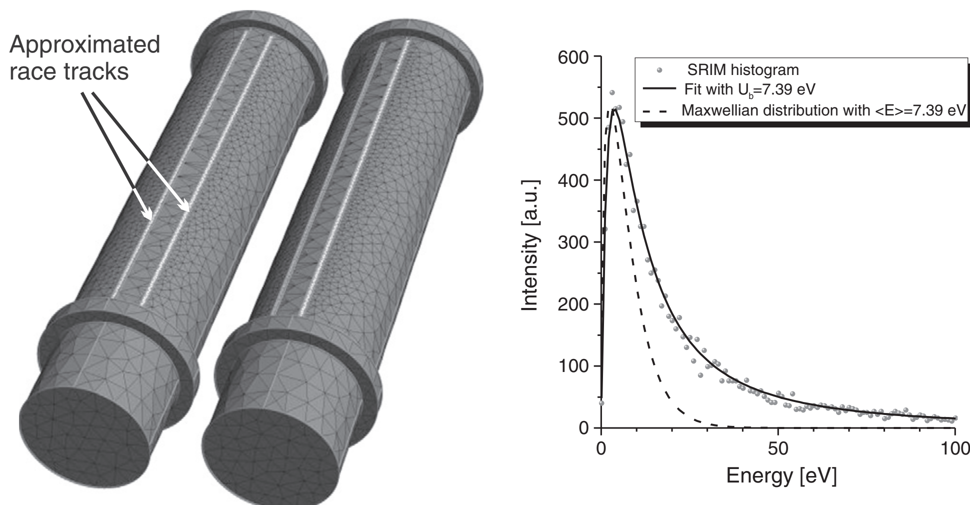

Fig. 2. Locations of sputter particle sources on rotatable targets (left) and energy distribution of sputtered particles in the case of Nb as target material (right).

Download English Version:

https://daneshyari.com/en/article/8028080

Download Persian Version:

https://daneshyari.com/article/8028080

Daneshyari.com